Topographically Controlled Mesoscale Flow Anomalies on the Continental Shelf off Southern Sierra Leone and Liberia

DAVID W. MCGRAIL

Department of Oceanography, Texas A&M University, College Station 77843

(Manuscript received 4 April 1978 in final form 15 August 1978)

ABSTRACT

Analyses of records from current meters moored on the continental shelf off Liberia and southern Sierra Leone during March and April of 1972 indicate that the flow at that time was dominated by low-frequency oscillations in the near-inertial and sub-inertial range. However, dynamic velocities calculated from hydrocast and XBT data using standard geostrophic approximations were frequently incorrect in both magnitude and sign when compared to the appropriate portions of the velocities recorded by the proximal current meters. Horizontal plots of the topography on isothermal surfaces in areas where the ageostrophic flow was found revealed that the density field there was significantly deformed over small (radius of curvature as small as 2 km) bathymetric elements. Orientation of the principal axis of variance for the current meter records also suggests that the mesoscale flow undergoes strong topographic steering on this low-latitude shelf.

1. Introduction

The work reported here was motivated by a desire to understand the coupling between fluid motions and sediment distribution on the stretch of continental shelf between Cape Palmas and St. Ann's Shoal (Fig. 1) in northwest Africa. At the outset, the problem appeared to be reduced to the simplest case one might reasonably expect in the natural setting. The area is unique in its lack of storms, negligible wind stress and readily identifiable modern sedimentary deposits of relatively simple geometry. In addition, there was available a myrid of complementary hydrographic and geologic data from the area to facilitate the investigation.

In a similar study (McGrail, 1977) of the region to the north, the continental shelf off Guinea Bissau, Guinea and northern Sierra Leone, a simple technique for calculating the vertical distribution of dynamic velocity between hydrographic stations was developed as an aid in depicting the vertical structure of the currents. This approach seemed reasonable since the time and length scales appropriate to the sedimentary features of interest were comensurate with those of geostrophic flow phenomena and the strong stratification implied the importance of baroclinicity. The technique consists of integrating the thermal wind equation up the water column from an assumed velocity of zero at the bottom. It is equivalent to calculating dynamic heights relative to a sloping reference level. The method yielded surface velocities consistent with historical observations (~30–50 cm s^{-1} to the southeast) in that area. More importantly, it revealed the presence of a poleward flowing subsurface current over the very region on the outer shelf in which sediment was found to be migrating to the northwest.

During the experiment on which the present study is based, several cross-shelf transects with multiple XBT and hydrographic stations were run within a kilometer of current meter moorings. This circumstance permitted comparison of velocities determined by the above method at the level of the current meters with those actually measured by the instruments. It was assumed *a priori* that the measured velocities would have greater magnitudes because the dynamic method neglects inertial and viscous terms in the boundary layer and the possible contribution of barotropic components of flow. Contrary to expectations, the magnitude of the calculated velocities was up to five times that recorded by the current meters. Worse yet, calculated surface velocities exceeded those indicated by ship drift by as much as a factor of 20. Even more perplexing, the velocities obtained from integration of the thermal wind equation frequently possessed a directional sense opposite to that recorded by the current meters during the time of the stations from which the calculations were made.

The peculiarity of these results necessitated a thorough analysis of the flow regime on this shelf. This report is comprised of that analysis, development of an alternative method for approximating the velocity distribution, and an example of its application.

Data and samples used in this study were collected

0022-3670/79/020327-10$06.50

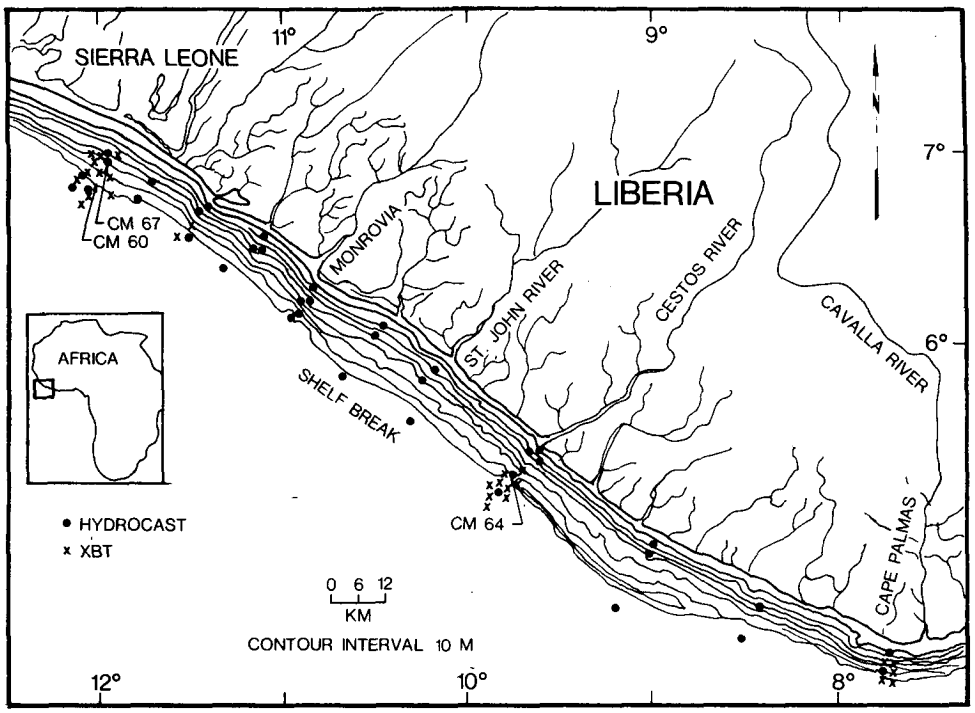

FIG. 1. The area of investigation with sample locations. The letters CM connote current meter.

on cruise TR 112 of the University of Rhode Island's R/V *Trident* during March and April of 1972. These data include records from three moored current meters, XBT traces, temperature and salinity determinations from hydrocasts, detailed bathymetric profiling, high-resolution low-penetration sub-bottom profiles, suspended sediment samples, and samples of the surface sediment from the continental shelf.

Though considerable attention has been focused on the shelf dynamics of the Gulf of Guinea and northwest Africa north of Dakar, the area between has been largely ignored. Berrit (1961,1962), using data collected from merchant vessels passing through the Gulf of Guinea and along the northwest African Coast, characterized the region north of Liberia as belonging to the boreal regime. There, upwelling takes place in the boreal winter as far south as Guinea Bissau. He states that the Gulf of Guinea, on the other hand, belongs to the austral regime and exhibits upwelling as far west as Cape Palmas. According to Berrit (1961,1962) the area between Cape Verga in Sierra Leone and Cape Palmas in Liberia is a region of transition characterized by an absence of upwelling the year round.

Circulation on the continental shelf in the Gulf of Guinea is reported (Lemasson and Rebert, 1968; Le Floch, 1970) to consist of a shallow, primarily eastward flowing surface current and a primarily westward flowing subsurface current which extends down to about 90 m. Lemasson and Rebert (1973) investigated the temporal stability of the current system in the Gulf of Guinea and tried to delineate the western terminus of the Guinea undercurrent using over-the-side current meters in conjunction with temperature, salinity, oxygen and nutrient measurements. They found that the undercurrent was almost always present but exhibited considerable variation in magnitude. However, they were unable to determine whether or not the undercurrent rounded Cape Palmas. Gerard *et al.* (1965), using subsurface drogues, did observe a northwesterly flow of 29 cm s^{-1} at a depth of 60 m, beneath southeastward flowing surface water at a location over the continental slope southwest of Cape Palmas.

More recently, Houghton (1976) and Houghton and Beer (1976) have reported that upwelling in the Gulf of Guinea is poorly correlated with the local wind regime. They also report the presence of trapped waves in the waters off Ghana which have a period of about 14 days. Although the dispersion characteristics of the waves are consistent with those of a shelf wave, those investigators offer several lines of evidence to suggest that the waves are primarily baroclinic.

In the previous study (McGrail, 1977) of the shelf off northern Sierra Leone, Guinea and Guinea Bissau, the temperature distribution and demonstrable recent sediment transport were used to deduce the presence of a poleward flowing, shelf edge current. The northwesterly flowing current, designated the Canary Countercurrent was found to exist beneath

the southeasterly flowing waters of the Canary Current. Carder *et al.* (1974), using the foregoing and a preliminary analysis of some of the same data used in this study, concluded that a similar two-level flow also exists off Liberia and southern Sierra Leone. That position was somewhat mitigated in McMaster *et al.* (1977).

2. Current meters, description and analyses of records

Records from three Geodyne model 102 current meters which had been moored at the locations indicated in Fig. 1 were employed in this investigation. The sampling rate for these had been set so that 2.4 min of data were recorded at intervals of 5 min. Basic data regarding the meters appears in Table 1. Meter 60 returned direction only. The current meter records had already been converted to 1 h vector averages by the time they were obtained for this study.

Power spectra of the two complete records were calculated by means of a fast Fourier transform using the method described by Weisberg (1974). The brevity of the records, however, precluded statistically significant resolution of the energy density in the low-frequency bands of the spectrum. For example, to reduce the error of the estimate to 10% for a bandwidth of 7.7×10^{-3} cycles per hour (cph) the inertial frequency at latitude 5.25° N (that of meter 64), a record 545 days long would be required for the sampling rate of one per hour.

TABLE 1. Current meter station data.

Meter	Station depth (m)	Meter depth (m)	Dates	Record length (h)
67	68	56	3/11–3/23	287
64	85	75	3/26–4/23	680
60	89	71	3/11–3/23	268

Even though the power spectra from these records were insufficient to resolve the energy densities into narrow frequency bands, it may be reasonably inferred from them that most of the variance of the records occurs in the inertial frequency range and below with some modulation at the frequency of the semidiurnal tide. The raw power spectrum for the north-south components of the record from current meter 63 (Fig. 2) exemplifies these characteristics.

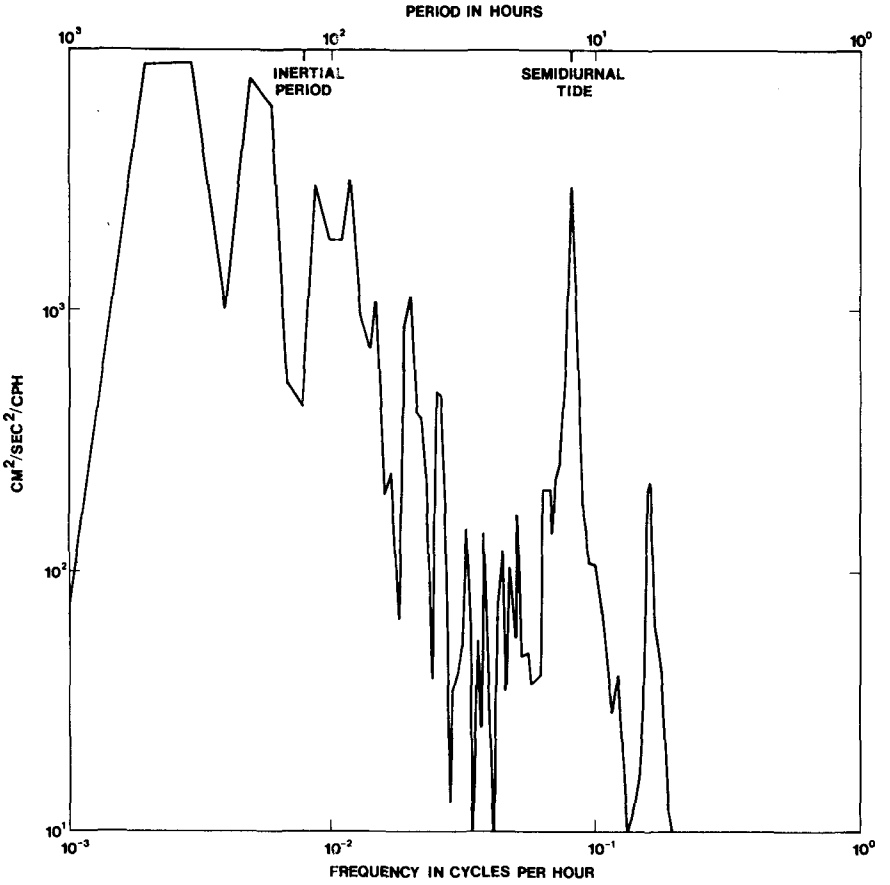

FIG. 2. Raw power spectrum of the north-south components of current meter 64 with two degrees of freedom.

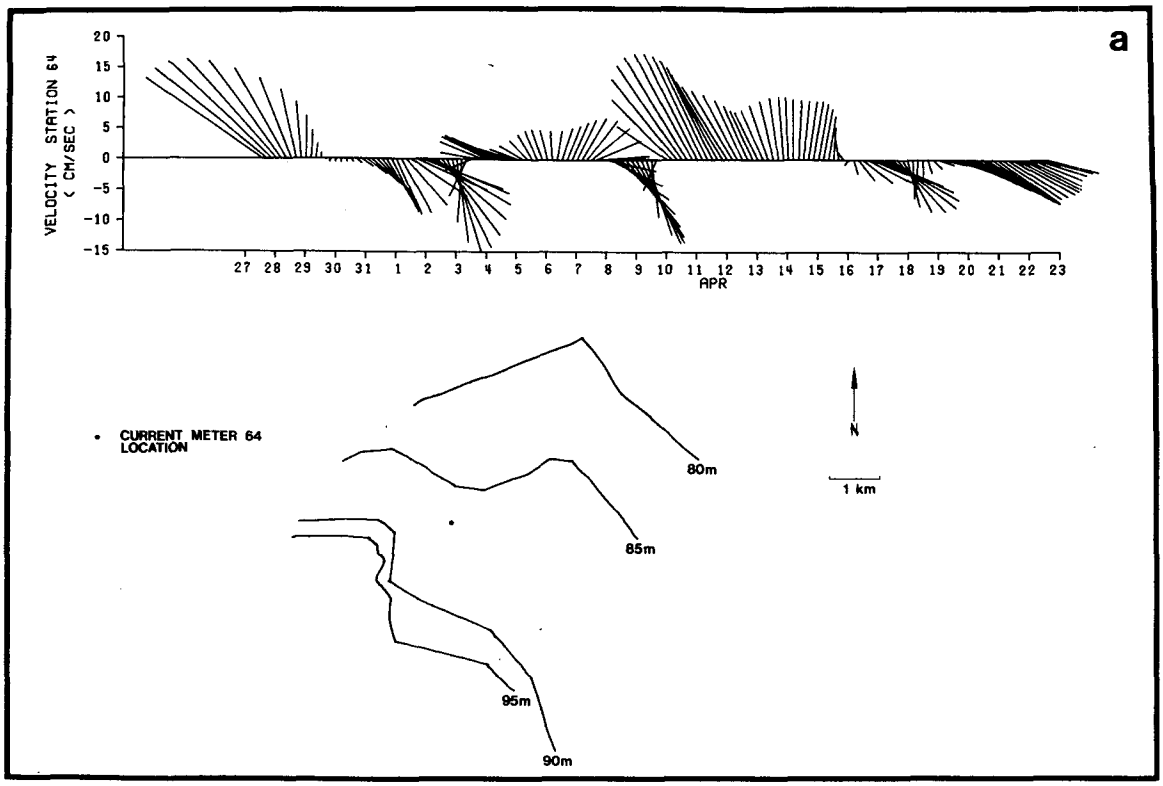

FIG. 3a. Time series plot of low pass filtered record from current meter 64. Vectors are plotted every 4 h. Location of the current meter relative to local bathymetry is shown below the time series.

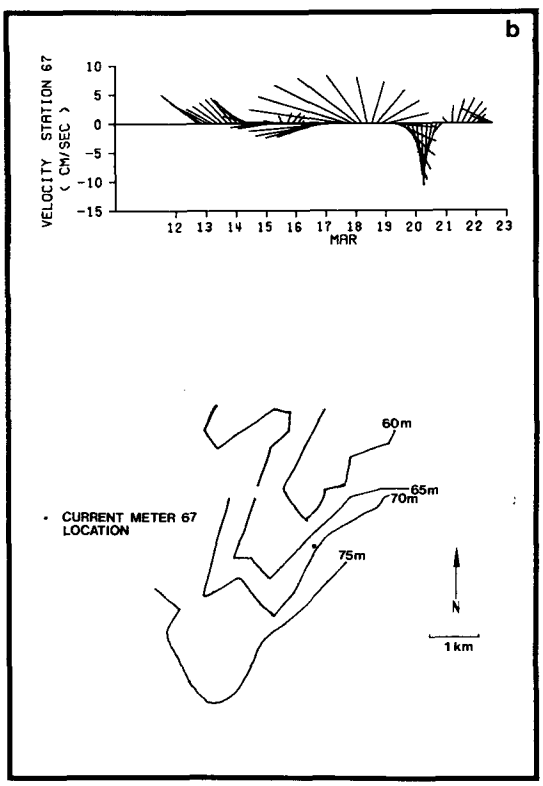

FIG. 3b. Time series plot of low pass filtered record of meter 67 as in Fig. 3a.

In order to determine whether the current meter records did or did not contain information about the flow which could account for the peculiar results obtained in the dynamic analysis, they were low-pass filtered and plotted. The filter used was a Gaussian function with a standard deviation of 8 h and a frequency response of 0.11 at the diurnal frequency. After smoothing, the records were plotted as vectors with the origin moving along a time axis in 4 h increments (Fig. 3).

The graphic display of meter 64's record (Fig. 3a) revealed an oscillatory flow with a remarkable degree of polarization along a northwest-southeast axis. Careful examination of the plot suggests that the elliptical rotation of the vectors is almost exclusively clockwise. The period of that rotation is not as unambiguously shown in the plot because there appear to be several slightly out-of-phase cycles of varying amplitude present. There is some evidence of a 7-day periodicity in the records. Note, for example, the cycle extending from 3 to 10 April. This would suggest that the frequency of the oscillations lies well into the subinertial range for the location of the current meter since the inertial period there is 5.4 days.

The time series plot of the record from current meter 67 (Fig. 3b) is significantly different from that of meter 64 and is far more enigmatic. Instead of rotating through ellipses in a clockwise sense as they

did in the record of meter 64, these vectors, with the exception of those in the 2-day period centered about 20 March, oscillate between a northwesterly and northeasterly orientation. Some of the fluctuations recorded by current meter 67, including the most energetic, have a periodicity very near 4.4 days, the inertial period for the latitude of the mooring (6.5° N). However, there is no indication of the longer period motions seen in the record of meter 64.

A method for extracting information from the fluctuating portion of the record has been suggested by Freeland *et al.* (1975). It consists of solving for the eigenvalues of the variance tensor and determining the orientation of the principal axis. The eigenvalues are roots of

$$(\overline{u^2} - \lambda)(\overline{v^2} - \lambda) - \overline{uv}^2 = 0,$$

where u is the east-west component of velocity, v the north-south component of velocity and the overbar denotes time average. The Orientation of the major axis is given by

$$\theta = 0.5 \tan^{-1}[\overline{uv}/(\overline{v^2} - \overline{u^2})].$$

The angle θ is obtained as a compass direction directly from this form of the computation.

As might be expected from a visual inspection of current meter 64's record (Fig. 3a), the variance is maximized along an axis trending northwest (304°)–southeast (124°) (Fig. 4). This orientation of the principal axis is parallel to the large-scale bathymetric trend of the shelf. The degree of polarization of the flow along that trend is evidenced by the fact that 86% of the variance in the record can be accounted for by that orientation of the principal axis. At the time and location of current meter 64's mooring, then, the flow was dominated by a motion of subinertial frequency in which the current underwent eliptical, clockwise rotation such that strong alongshore flow alternated with weak cross-shelf flow. In the absence of any apparent local forcing mechanism, the logical inference is that the above observations are due to the passage of free shelf waves which probably emanated from the Gulf of Guinea.

It is the orientation of the principal axis of variance for current meter 67's record, however, which suggests the cause of problems experienced in the dynamic analysis. That axis trends nearly east (78°)–west (258°) tangential to the adjacent 60 m isobath as it curves around the nose of a submarine ridge (Fig. 4). Reexamination of the plot of meter 67's record (Fig. 3) reveals that most of the vectors are parallel to the 60 m isobath either across the nose of the ridge or along its southeastern flank. This implies that the flow at the height of meter 67 (56 m) was significantly deformed by a bathymetric element with a radius of only about 1 km. Scaling the

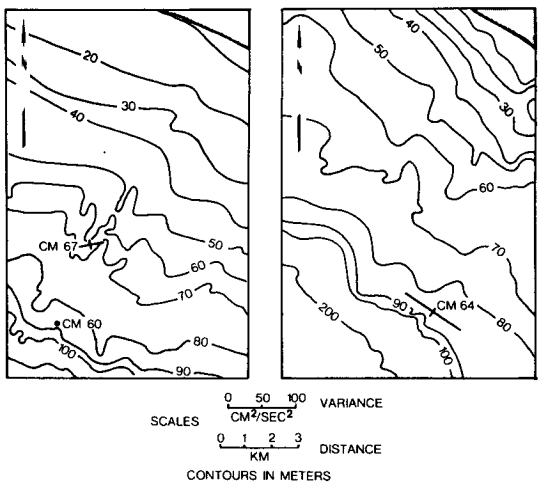

FIG. 4. Principal axis of variance plots for the records of meters 64 and 67. The origin is centered at the location of each mooring relative to the local bathymetry.

flow with a characteristic velocity of 10 cm s^{-1} and a length of 1 km produces a Rossby number of just over 6 indicating that inertial accelerations are far from negligible. If the density distribution of the water column is adjusted to such a deformation of the flow field, the geostrophic component of the baroclinic motion would balance only a fraction of the resulting pressure gradient.

3. Horizontal temperature distribution

The means of examining the relationship between the internal field of mass and the bathymetry was provided by the unusual circumstances of having data from over 30 XBT and hydrocast stations located in a small (10 km × 25 km) rectangular area surrounding current meter 67's mooring. Such close station spacing made it possible to compare the form of the density distribution with that of the large-scale geomorphic features of the bottom. During the course of this work, it was found that over 90% of the density variations in the region were due to thermal contrasts. The nature of the density distribution could therefore be shown by a simple plot of the temperature distribution. The best method for representing the relationship between the temperature distribution and the bottom configuration proved to be plotting the topography on an isothermal surface, then overlaying it on the contoured bathymetry.

The first surface plotted, 20°C, was the deepest present at every station and therefore the most likely to exhibit deformation if it existed. Fig. 5 gives striking evidence of the complementary forms of the bottom and the 20°C surface. The intensity of the topographic deformation is reflected by the fact that there is over 20 m of relief on that surface. It seemed

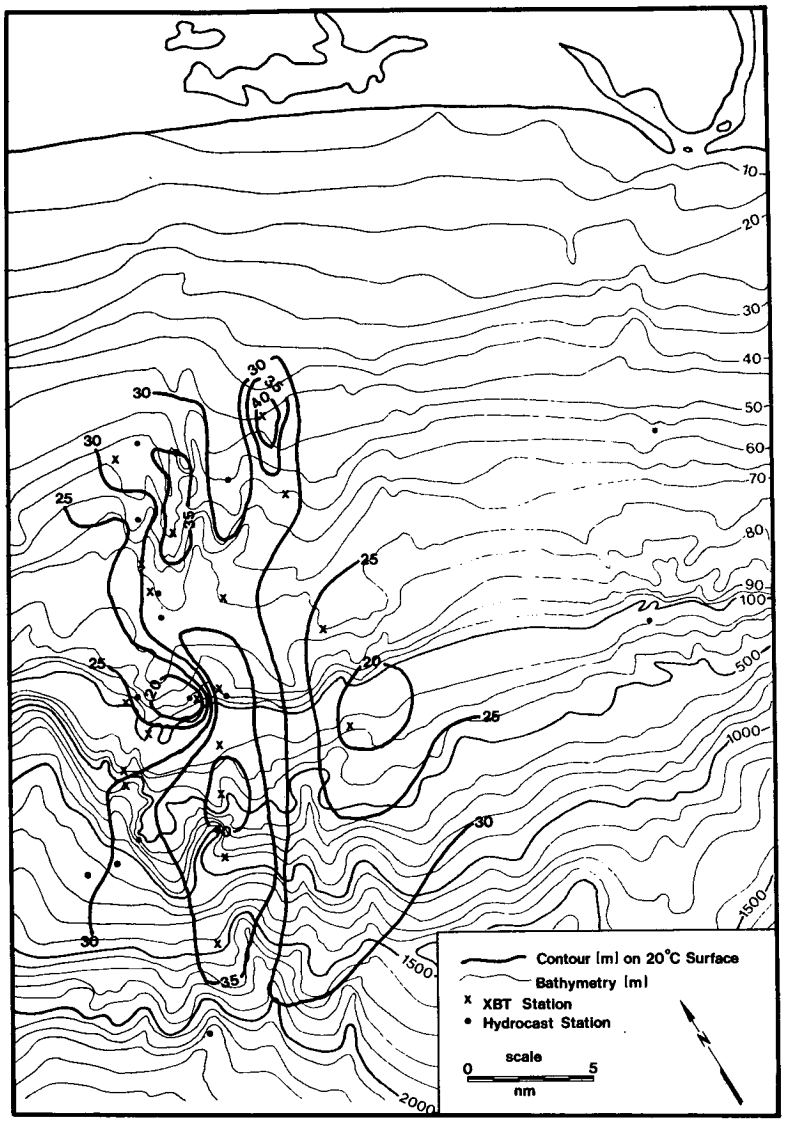

FIG. 5. Topography of the 20°C isothermal surface superimposed on bathymetry. Current meter 67 was moored on the ridge outlined by the 35 m contour of the 20° surface at left center of the figure.

likely that the deformation might have penetrated the thermocline because the topographic effect was so strongly imprinted on the 20°C surface which lay at the base of the thermocline. Fig. 6, a plot of the 25°C surface (top of the thermocline), offers ample evidence that the inertial accelerations caused by flow around crenelations in the bottom topography resulted in deformation of the density distribution which did extend through the thermocline.

Though the station density at this location is unusually high, the data are insufficient in both number and uniformity of distribution to permit contouring of the isothermal surfaces with the fine detail of the bathymetry. This difference in control, coupled with the possible presence of progressive internal waves, preclude comparison of the topography on the bottom and on the isothermal surfaces on an element by element basis. The temperature distribution around the ridge on which meter 67 was moored (left center in Figs. 5 and 6) is, however, illustrative of the response of stratified flow to irregularities in the bottom topography. From the XBT station on the nose of the ridge it was found that the 20°C surface was downwarped 8–10 m relative to its position in adjacent stations. Similarly, the 25°C surface at that station was found at 29 m, more than 14 m below its depth in nearby stations. A simple explanation of this distribution is that as the shelf waters flowed along the tightly curving isobaths of the ridge, centrifugal acceleration displaced the

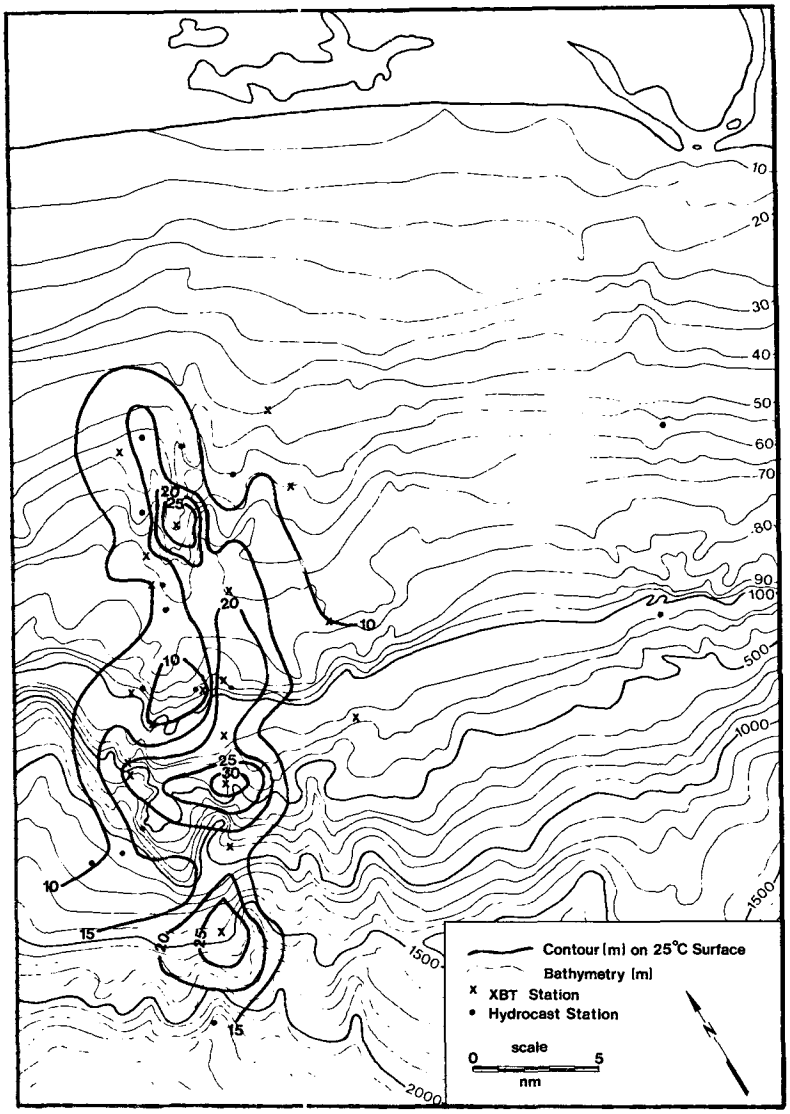

FIG. 6. Topography of the 25°C isothermal surface plotted over bathymetric contours.

denser waters below the thermocline further from the center of curvature than the less dense surface water. That resulted in a downwarping of the thermocline over the crest of the ridge. The failure of the dynamic technique can therefore be explained by the fact that the flow is rendered locally ageostrophic through strong inertial accelerations induced by topographic steering.

4. A correction for centripetal acceleration

In the previous study (McGrail, 1977), velocity profiles between hydrographic stations were obtained by integrating the velocity shear. This method starts with the "thermal wind equation" (Neumann and Pierson, 1966) which, in an arbitrary coordinate system with z positive down and n normal to the direction of flow, is

$$\frac{\partial v}{\partial z} = g\rho_0^{-1}f^{-1}\frac{\partial \rho}{\partial n}, \tag{1}$$

where v is the velocity, f the Coriolis parameter, ρ_0 a reference density and g the gravitational acceleration. To obtain the velocity at any height ($z = h$) above the bottom ($z = H$), Eq. (1) was integrated up from the bottom subject to the boundary condition that $v(H) = 0$. Therefore,

$$v(z)_{z=h} + c = g\rho_0^{-1}f^{-1}\int_H^h \frac{\partial \rho}{\partial n}\,dz. \tag{2}$$

The constant of integration c in (2) is the depth-

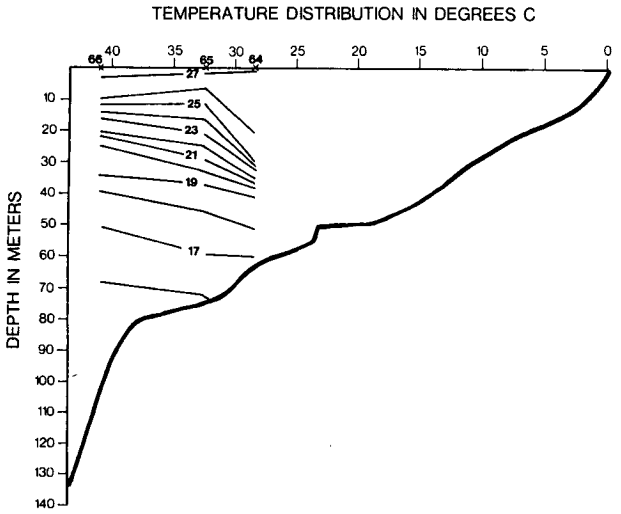

FIG. 7. Temperature distribution on a transect adjacent to current meters 60 and 67 (see Fig. 1 for locations). Note the steep downward slope of the isotherms between stations 64 and 65. Distances at the top are in kilometers from shore.

independent (barotropic) component of the velocity. Without some absolute measure of the flow, its value is indeterminate. In the present study, it was assumed that c could be found by obtaining the difference between the integrated velocity shear at the height of the current meter and the velocity recorded by the instrument (appropriately averaged) during the period of hydrographic observations. A correction to v for boundary layer dissipation would also have been given by this method. Implementation of the method, however, proved to be impractical because of the topographic deformation of the flow. The error in (2) induced by neglect of the inertial term was so large and the barotropic component so small that c was submerged in the uncertainties arising in calculations. It was therefore neglected.

The correction to (2) required to find the geostrophic velocity is of the order of the contribution from the inertial acceleration. Since the Rossby number ϵ is an estimate of the ratio of inertial to Coriolis acceleration, the product

$$\epsilon v_1 = v_1^2 L^{-1} f^{-1}, \tag{3}$$

where v_1 is the geostrophic velocity and L a scaling length, is of the form and order of the desired correction. Adding the correction from (3) to the left side of (2) yields,

$$v_1 + v_1^2 L^{-1} f^{-1} = g f^{-1} \rho^{-1} \int_H^h \frac{\partial \rho}{\partial n} dz. \tag{4}$$

As long as the pressure field is entirely baroclinic, (4) is equivalent to the "gradient wind equation" of meteorology (Holton, 1972). If both sides of (4) are multiplied by f, it can be seen that the pressure gradient is balanced by acceleration of bathymetrically deviated flow. If it is assumed that the bathymetric contours are not closed, L may be assigned a sign depending on whether the contours are concave ($+L$) or convex ($-L$) with respect to n. As long as the Rossby number lies in the interval $-1 > \epsilon < +1$, the centripetal acceleration is merely an additive or subtractive correction to the velocity and the direction of flow [sign of the solution to the quadratic (4)] can be determined from the sign of the pressure gradient. If, however, ϵ lies outside that interval, the centripetal acceleration is the dominant term and the direction of flow is indeterminate since flow in either direction produces the same centripetal acceleration. In that case, the sign of the pressure gradient depends only on L.

5. Application of the corrected equation to the data

Of the many hydrographic sections occupied on the shelf off Liberia and Sierra Leone, seven were run within 5 km or less of the moored current meters. One of these sections is used here to demonstrate the application of (4) to the data. It was chosen for the clarity with which it exhibits the effects of topographic steering in the presence of relatively simple bathymetry. It should be borne in mind when evaluating these data that the Coriolis parameter at 7° N is only 18% of that at 45° N. Therefore, in order to achieve a geostrophic balance with a given pressure gradient, the velocity at 7° N must be nearly six times greater than that required at 45° N. Similarly, at Cape Palmas (4° N) the velocity must be almost nine times as great as that required in middle latitudes.

The section, comprised of stations 64, 65 and 66, traverses the same ridge considered previously. The temperature distribution inferred from these three stations appears in Fig. 7. Since the density variations of the water here is almost totally temperature-dependent, the steep northeastward slope of the isotherms implies flow to the northwest (into the page). Solving (2) for a position midway between stations 64 and 65 yields a surface velocity in excess of 350 cm s^{-1} to the northwest.

The flow recorded by current meters 60 and 67 for the 12 h period centered at the time of station 65 is shown in Fig. 8. Though it recorded no speed, current meter 60 did record a generally southeasterly flow for the period. The record of meter 67, however, indicates that the flow for the same period was to the northeast. Since these meters were at approximately the same depth (~60 m), this represents rather significant divergence of flow. The vector average for this 12 h segment of meter 67's record is 7 cm s^{-1} toward 17° T. The point here is that both ship drift and current meters indicate flow with a directional sense opposed to that obtained by solution of (2).

The normal components of velocity through the plane connecting the three stations were recomputed using (4). In practice, this involved solving (2) at horizontal intervals of 0.5 km across the section, then iterating using (4) to correct for centripetal acceleration. Isotachs of the corrected velocity obtained from the roots of (4) having the same directional sense as indicated by ship drift and current meters are shown in Fig. 9. In this case, the flow was convex with respect to n, and the radius of curvature L was quite small. The inertial term in (4) was therefore larger than the geostrophic velocity so that the pressure gradient would have been negative with flow in either direction.

6. Concluding remarks

Though the current meter records used in this study were too short to permit statistically satisfactory analysis, they do contain sufficient information to support some qualitative inferences regarding circulation over this low-latitude continental shelf. The flow recorded by the meter at the southern mooring possessed a shoreward directed mean velocity of less than 2 cm s^{-1} and was dominated by rather energetic oscillations at subinertial frequencies. These velocity fluctuations were characterized by elliptical clockwise rotation of the vectors having the major axis of variance oriented parallel to the general shelf trend. The characteristics exhibited by the oscillations in this record imply that they may be trapped shelf waves. Because the study area is straddled by the Intertropical Convergence Zone, no apparent local forcing mechanism exists to drive such waves. For that reason it is suspected that these are free shelf waves generated in and propagating out of the Gulf of Guinea. Low-frequency (0.07 cycle per day) oscillations have been observed there by Houghton and Beer (1976) and Houghton (1976).

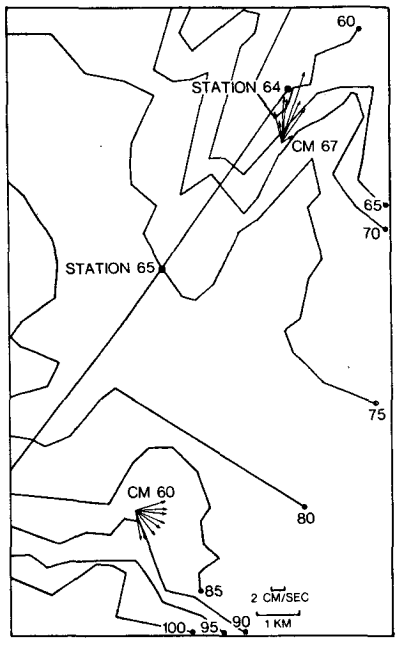

FIG. 8. Trackline between stations 64 and 65 plotted on detailed bathymetry. Note the convexity of the isobaths intersected by the trackline. Current roses are 1 h vector averages for six hours before and 6 h after the time of station 65. Vectors at meter 60 have a constant 5 cm s^{-1} speed because it returned direction only. Depths are in meters.

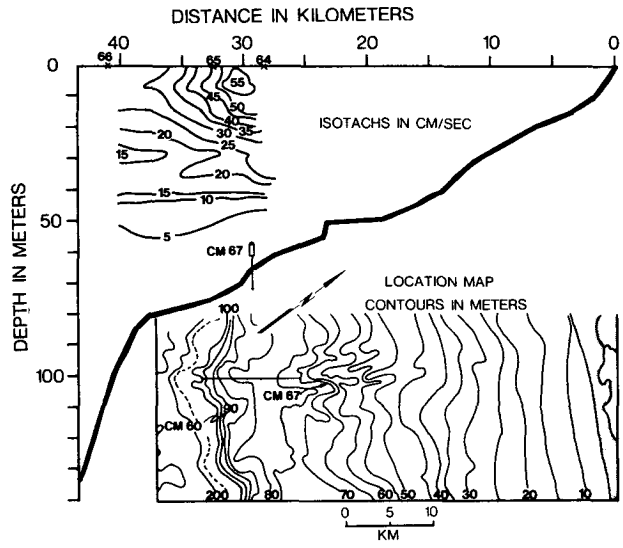

FIG. 9. Cross section is a plot of isotachs computed from temperature distribution in Fig. 7. Flow is to the southeast (out of the page). Map view is the location of the trackline between stations 64, 65 and 66. Note that the isobaths are convex toward the sea. Dashed contour is the shelf break at 135 m.

The most energetic velocity fluctuations recorded at the northern mooring site also exhibited elliptical clockwise rotation of the current vectors. However, at this location the oscillations occurred at the inertial frequency, were less energetic, and possessed a major axis of variance with an oblique orientation to the coastline. Also, the mean velocity was over 4 cm s^{-1} to the northwest. The loss of energy and increase in frequency in the dominant signal from south to north could result from a variety of circumstances. It could, for instance, be due to the brevity and asynoptic nature of the observations; that is, the northern mooring could have been terminated prior to the onset of an episode of shelf wave activity which dominated the motion during the period in which the southern mooring existed. That possibility seems rather remote in an area of such extreme meteorological stability. A more reasonable explanation is that interaction of the shelf waves with topography between the moorings (~300 km apart) resulted in both dissipation of energy and its leakage to a higher frequency inertial mode of motion.

Regardless of the origin of the observed velocity fluctuations, their long periods imply that the flow in this region should be quasi-geostrophic. Dynamic calculations using standard techniques to obtain velocities from station data indicate that this was often not the case. Horizontal plots of isothermal surfaces demonstrate quite clearly that this violation of expectation arises from topographic deformation of this flow by small bathymetric elements. Ridges and valleys possessing radii of curvature on the order of only 2 km exert a surprisingly large influence on the mass distribution of these shelf waters. The accuracy with which velocities were hindcast by means of (4) and the orientation of the velocity vectors recorded by the northern current meter further strengthen the inference that the flow was topographically controlled during the period of observations.

In part, the importance of the topographic steering in the dynamics of fluid motion on the shelf off Liberia and Sierra Leone is due to the low latitude of the area. The pressure gradient required to balance the centripetal acceleration of a curving flow is constant whether the deformation is at 5° or 50° of latitude. The error induced in calculating the velocity by neglecting inertial accelerations and making the geostrophic assumption is, however, nine times greater at 5° than at 50° because f at 5° is only 11% of that at 50°. The presence of topographic steering is therefore poignantly apparent in the case of this northwest African shelf but might escape notice on a midlatitude shelf.

Acknowledgments. Support for this study was supplied by the Office of Naval Research under Contract N000 14-68-A-0215-003 to the University of Rhode Island. The support of the Academic Computer Center and the Graduate School of Oceanography at the University of Rhode Island for computer time and facilities made available is gratefully acknowledged.

I am indebted to Dr. R. L. McMaster for the data and samples used in this study and for his encouragement through some very bleak hours on this project. Thanks are also due Drs. Randolph Watts, Phillip Richardson, Merton Ingham and Frank White for their helpful discussions on the vagaries of fluid mechanics during the course of this work.

The manuscript was reviewed by Takashi Ichiye and improved by adoption of his suggestions. William Cramer wrote and made available the programs used to filter, preprocess and plot the current meter records as "stick diagrams".

REFERENCES

Berrit, G. R., 1961: Contribution a la connaissance des variations saisonnieres dans le Golfe de Guinee: Observations de surface le longe des lignes de navigation: I. *Cah. Oceanogr.*, **13**, 715–727.

——, 1962: Contribution a la connaissance des variations saisonnieres dans le Golfe de Guinee: Observations de surface le longe des lignes de navigation: II. *Cah. Oceanogr.*, **14**, 633–643.

Carder, K. L., P. R. Betzer, and D. W. Eggiman, 1974: Physical chemical and optical measures of suspended-particle concentrations: Their intercomparison and application to the West African shelf. *Suspended Solids in Water*, Gibbs, R. J., Ed, Plenum Press, 173–193.

Freeland, H. J., P. B. Rhines and T. Rossby, 1975: Statistical observations of the trajectories of neutrally buoyant floats in the North Atlantic. *J. Mar. Res.*, **33**, 383–404.

Gerard, R., R. Sexton, and P. Mazeika, 1965: Parachute drouge measurements in the eastern tropical Atlantic in September 1964. *J. Geophys. Res.*, **70**, 5696–5698.

Houghton, R. W., 1976: Circulation and hydrographic structure over the Ghana Continental Shelf during the 1974 upwelling. *J. Phys. Oceanogr.*, **6**, 909–924.

——, and T. Beer, 1976: Wave propagation during Ghana upwelling. *J. Geophys. Res.*, **81**, 4423–4429.

Holton, J. R., 1972: *An Introduction to Dynamic Meteorology*. Academic Press, 319 pp.

Le Floch, J., 1970: Measures differentielles de conrants an large de la Cote d'Ivoire. *Cah. Oceanogr.*, No. 8, 781–799.

Lemasson, L., and J. P. Rebert, 1968: Observation de courents sure le Plateau Continental Ivoirieu—Mise en evidence d'un sons-courent. Doc. Sci. Prov., No. 22, CRO Abidjan.

—— and ——, 1973: Les courant marins dans le Golfe Ivoirieu. *Cah. ORSTOM, Ser. Oceanogr.*, **11**, No. 1, 67–95.

McGrail, D. W., 1977: Sedimentologic and physical oceanographic evidence of a shelf edge counter current off Guinea Bissau, Guinea and Sierra Leone. *J. Sed. Petrol.*, **47**, 915–925.

McMaster, R. L., P. R. Betzer, K. L. Carder, J. Miller, and D. W. Eggiman, 1977: Suspended particle mineralogy and transport in water masses of the West African Shelf adjacent to Sierra Leone and Liberia. *Deep-Sea Res.*, **24**, 651–665.

Neumann, G., and W. J. Pierson, 1966: *Principles of Physical Oceanography*. Englewood Cliffs, 545 pp.

Weisberg, R. H., 1974: The nontidal flow in the Providence River of Narragansett Bay. Ph.D. thesis, University of Rhode Island, 127 pp.